Indian Journal of Pure & Applied Physics
Vol. 54, March 2016, pp. 193-198

Growth, spectral, thermal, mechanical, linear and nonlinear optical studies of divalent metal ions doped zinc tris-thiourea sulphate single crystals

K Kanagasabapathy[1], G Gowri Shanmugapriya[2], S Vetrivel[3] & R Rajasekaran[4]

[1]A A Government Arts College,Villupuram 605 602, India
[2]VRS College of Engineering and Technology, Arasur 607 107, India
[3]Government Arts College, Tiruvannamalai 606 603, India
[4]Kolanjiappar Government Arts College, Vriddachalam 606 001, India

Received 20 January 2015; accepted 4 November 2015

Zinc tris-thiourea sulphate (ZTS) and divalent metal ions (Cd^{2+} and Ni^{2+}) doped zinc tris-thiourea sulphate materials are synthesized from aqueous solution and single crystals are grown from aqueous solution by slow evaporation technique. The unit cell parameters of the grown crystals are evaluated by single crystal X-ray diffraction analysis. The powder X-ray diffraction patterns are recorded and indexed for further confirmation of crystalline nature of grown crystals. The presence of functional groups in the grown crystals has been confirmed by FTIR analysis. The incorporation of cadmium and nickel ions entered into ZTS crystals is confirmed from SEM-EDX analysis. TGA/DTA thermal analyses revealed that the materials have good thermal stability. Mechanical behaviour have been studied using Vicker's microhardness measurements. *UV-visible* transmission spectra have been recorded in the spectral range 200-900 nm to find the cut-off wavelength and optical band gap E_g of grown crystals in non-linear applications. The nonlinear optical properties of pure and doped ZTS crystals were confirmed by Kurtz Perry powder method using Nd:YAG laser source.

Keywords: Growth from solution, X-ray diffraction, FTIR, Second Harmonic Generation, Nonlinear optical material

1 Introduction

In the recent years, the research is focused on semi-organic NLO material crystal in order to obtain superior NLO crystal by combining the advantages of organic and inorganic materials. The semi-organic NLO materials have been attracting much attention due to high nonlinearity, chemical flexibility, high mechanical and thermal stability and good transmittance. Among the semi-organic NLO materials, metal-complexes of thiourea family have been investigated actively[1]. Zinc tris-thiourea sulphate (ZTS) is an interesting semiorganic nonlinear optical (NLO) material[2]. Metal ions doped materials are currently receiving a great deal of attention due to the rapid development of laser diodes[3,4]. Doping influences the mechanical, electrical, optical properties and surface morphology depending upon the nature of the host material and the dopant[5,6]. The effect of metal doping on the physical and NLO properties of potassium hydrogen phthalate (KHP) and zinc thiourea sulphate (ZTS) crystals have been studied[7,8].

In the present investigation, attempts have been made to further improve the crystalline perfection and to study the influence of divalent metal ions (Cd^{2+} and Ni^{2+}) doping on the physicochemical properties of ZTS crystals grown by slow evaporation method from aqueous solution and its structural, FTIR, optical, mechanical and thermal behavior have been reported.

2 Experimental Procedure

ZTS compound was synthesized by stoichiometric incorporation of analar grade thiourea (99% Merck) and zinc sulphate heptahydrate (99% Merck). Thiourea and zinc sulphate heptahydrate were taken in the ratio of 3:1 and were dissolved in deionised water of resistivity 18.2 MΩcm. The ZTS compound was prepared according to the following reaction,

$$3(CH_4N_2S) + ZnSO_4.7H_2O \rightarrow Zn[(CH_4N_2S)]_3 \cdot SO_4 + 7H_2O \quad \ldots (1)$$

The synthesized salt was further purified by repeated recrystallization process. Using the purified ZTS, saturated growth solution was prepared and allowed it for slow evaporation. Good optical quality single crystal with regular shape and size 11×9×6 mm^3 was harvested within 20 days. For the growth of

*Corresponding author (E-mail: kksaba98@gmail.com)

Cd^{2+} doped ZTS crystal, 1 mol% of cadmium sulphate [$3CdSO_4.8H_2O$] was added to the solution of ZTS and single crystals of size 10×8×7 mm^3 with good transparency were grown in 35-40 days. For the growth of Ni^{2+} doped ZTS crystals, 1 mol% of nickel chloride [$Nicl_2.6H_2O$] was added to the solution of ZTS, single crystals of size 10×7×7 mm^3 with good transparency were grown in 35-40 days. The as-grown crystals of pure and metal ions doped ZTS crystals are as shown in Figs 1(a-c) respectively.

3 Material Characterization

The grown single crystals were subjected to single crystal XRD studies using a Kappa ApexII Nonius CAD4 diffractometer. Powder XRD patterns of the grown crystals were recorded using Bruker Powder X-ray diffractometer. FTIR spectrum of pure and metal ions doped ZTS was recorded by using an AVATAR 360 FTIR spectrometer in the wave length range 400-4000 cm^{-1}. Energy dispersive X-ray spectroscopy (EDX), a chemical microanalysis technique was performed on the grown crystals in conjunction with SEM using a JEOL JSM 5610 LV Scanning Electron Microscope with an accelerating voltage of 20 kV. In order to estimate the thermal behaviour, simultaneous thermogravimetric analysis and differential thermal analyses of pure and doped ZTS were carried out by TG/DTA instrument 6300, SII Nanotechnology Inc. Japan, Thermal Analyzer in the temperature range: RT to 800 °C (SiC furnace). The microhardness studies were carried out on the grown crystals using Vicker's Microhardness tester. The optical transmission of the crystal was recorded using VARIAN 5000 *UV-Vis-NIR* spectrophotometer in the wavelength region 200-900 nm. The nonlinear optical property of ZTS and Metal ions doped ZTS compound was confirmed by shining Nd:YAG laser of wavelength 1064 nm.

4 Results and Discussion

4.1 Structural analysis

4.1.1 Single crystal X-ray diffraction analysis

Single crystal X-ray diffraction studies of pure and 1 mol% divalent metal ions doped ZTS crystals were carried out using and their unit cell parameters are : a = 11.14 Å, b=7.77 Å, c = 15.50 Å, cell volume = 1341.65 $Å^3$, α = β = γ = 90° for ZTS crystal and a = 11.17 Å, b= 7.78Å, c = 15.53 Å, cell Volume = 1349.59 $Å^3$ and α = β = γ = 90° for 1mole% of Cd^{2+} doped ZTS and a = 11.16 Å, b= 7.78Å, c = 15.53 Å, cell Volume = 1349.59 $Å^3$ and α = β = γ = 90° for 1mole% of Ni^{2+} doped ZTS crystals. All the grown crystals belong to orthorhombic system with space group $Pca2_1$ and point group mm^2. The cell parameter values are in good agreement with the data available in JCPDS (76-0778) for pure ZTS with very nominal changes due to doping[9]. From single crystal X-ray analysis, the presence of dopant has marginally altered the lattice parameters without affecting the basic structure of crystal[4,10].

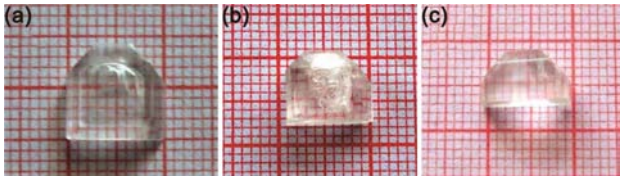

Fig. 1 – As grown crystals of: (a) ZTS (b) Cd^{2+} doped ZTS and (c) Ni^{2+} doped ZTS

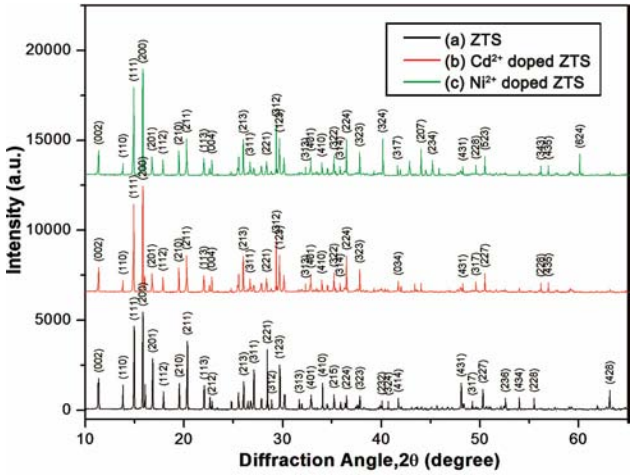

Fig. 2 – Powder XRD patterns of: (a) ZTS (b) Cd^{2+} doped ZTS (c) Ni^{2+} doped ZTS crystals

4.1.2 Powder X-ray diffraction studies

The Bragg's reflections in the powder XRD patterns (Fig. 2) were indexed for pure and divalent metal ions doped ZTS crystals. It is observed that the relative intensities have been changed and a slight shift in the peak position was observed as a result of doping. The most prominent peaks with maximum intensity of the XRD patterns of pure and doped specimens are quite different. These observations could be attributed to strain in the lattices. Appearance of sharp and strong peaks confirms the good crystallinity of the grown sample. The prominent well-resolved Bragg's peak at specific 2θ angle reveals the high perfection of the grown crystal. The observed values are in good agreement with the reported values[9].

4.2 FTIR spectral analysis

The FTIR spectra were recorded for as-grown crystals in the range of 400-4000 cm^{-1} is shown in Fig. 3. A close observation on FTIR spectra of pure and divalent metal ions doped crystals reveal that doping generally results in small shifts in some of the characteristic vibrational frequencies. It could be due to lattice strain developed as a result of doping. The broad envelope positioned in between 2750 and 3500 cm^{-1} corresponds to the symmetric and asymmetric stretching modes of NH_2 group. The CN stretching frequencies of thiourea (1089 and 1477 cm^{-1}) are shifted to higher frequencies of pure (1123 cm^{-1} and 1504 cm^{-1}), metal ions Cd^{2+} (1123 cm^{-1} and 1496 cm^{-1}) and Ni^{2+} (1123 cm^{-1} and 1496 cm^{-1}) doped ZTS crystals. The symmetric and asymmetric frequencies of CS stretching (740 cm^{-1} and 1417 cm^{-1}) are shifted to lower frequencies for pure (714 cm^{-1} and 1400 cm^{-1}) and metal ions doped (713 cm^{-1} and 1398 cm^{-1}) ZTS samples. These observations suggest that metal coordinate with thiourea through sulphur atom[4].

4.3 EDX analysis

The presence of cadmium and nickel in the doped specimen was confirmed by EDX analysis and the concentration of the incorporated Cd^{2+} and Ni^{2+} into the ZTS crystalline matrix can be clearly seen in Fig. 4(a-b). The surface analysis at different sites reveals that the incorporation of Cd/Ni was not uniform over the whole crystal surface. The amount of metal ions (Cd^{2+} and Ni^{2+}) incorporation into ZTS lattice is given in Table 1.

4.4 Thermo gravimetric analysis

TGA and DTA curves of pure and metal ions doped ZTS crystals are shown in the Fig. 5 (a-c) respectively. DTA curve of pure ZTS in Fig. 5a shows a sharp endothermic transition at 249.3 ºC. Further two endothermic peaks were observed at 300 ºC and 359.8 ºC. The first endothermic peak coincides with the melting point of the crystal is 249.3 ºC. TGA curve shows that the sample undergone a complete decomposition between 230 ºC and 800 ºC. The weight loss in the temperature range 231-280 ºC is due to the liberation of volatile substances like sulphur oxide in the compound[11].

DTA curve of Cd^{2+} doped ZTS in Fig. 5b shows three endothermic transitions with the first one at 236.9 ºC, the second at 301.9 ºC and the third at 361.9 ºC. The first endothermic peak coincides with the melting point of the crystal is 236.9 ºC. In the Cd^{2+} doped with ZTS, the melting point of ZTS

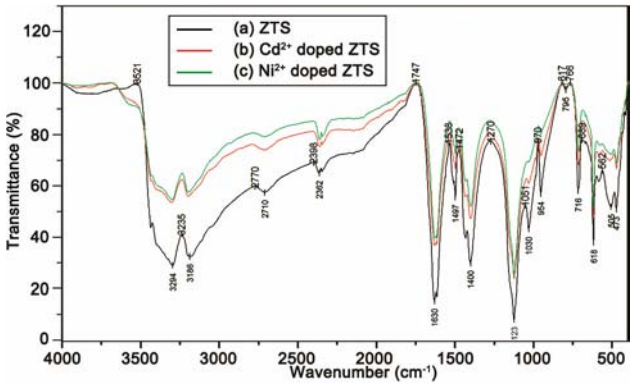

Fig. 3 – FTIR spectra of :(a) ZTS (b) Cd^{2+} doped ZTS (c) Ni^{2+} doped ZTS crystals

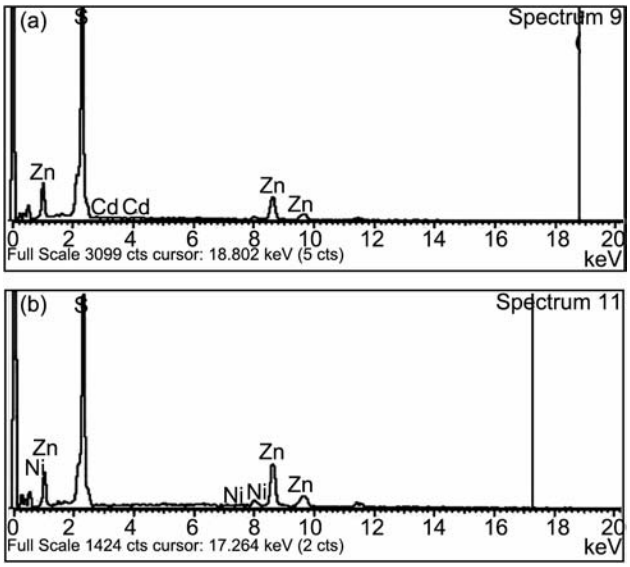

Fig. 4 – EDX spectrum of (a) Cd^{2+} doped ZTS and (b) Ni^{2+} doped ZTS crystals

Table 1 – EDX data for Metal ions doped ZTS crystals

Crystal	Element	Weight%	Atomic%
Cd^{2+}doped ZTS	S	54.44	70.95
	Zn	45.35	28.96
	Cd	0.21	0.08
Ni^{2+}doped ZTS	S	54.69	71.46
	Zn	44.64	28.35
	Ni	0.67	0.19

decreases slightly compared to pure ZTS. It is observed that maximum weight loss was observed in the temperature range 223.18 ºC - 381.2 ºC. A total weight loss of about 75.8% was occurred only at 600 ºC for Cd^{2+} doped ZTS crystal. This shows the thermal stability of the crystal.

DTA curve of Ni^{2+} doped ZTS in Fig. 5c shows three endothermic transitions with the first one at 241.97 ºC,

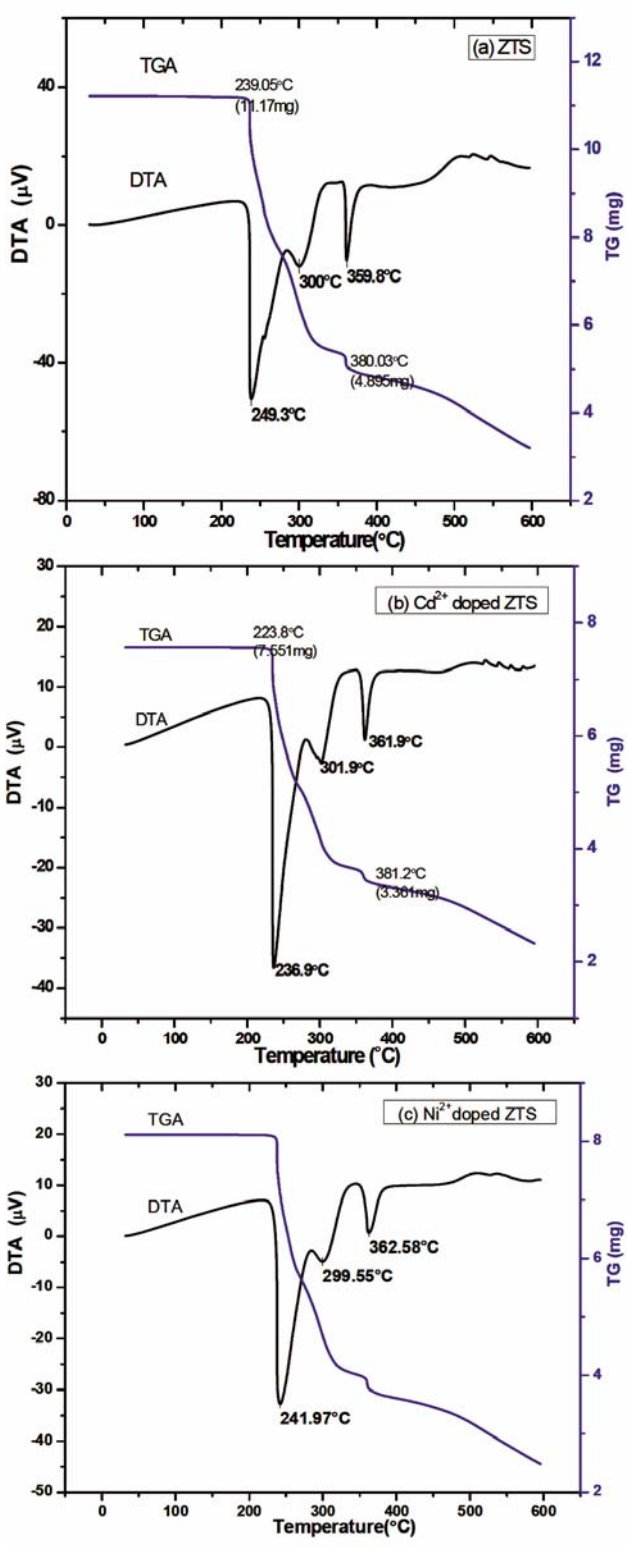

Fig. 5 – TGA/DTA curves of (a) ZTS, (b) Cd^{2+} doped ZTS and (c) Ni^{2+} doped ZTS crystals

the second at 299.55 ºC and the third at 362.58 ºC. The first endothermic peak coincides with the melting point of the crystal is 241.97 ºC. The melting point of pure ZTS was found to be 249.3 ºC[11]. When nickel chloride is doped with ZTS, the melting point decreases slightly. TGA curve shows that the sample undergoes a complete decomposition between 230 ºC and 800 ºC. The weight loss in the temperature range 231 ºC - 280 ºC is due to the liberation of volatile substances like sulphur oxide in the compound. There is no major weight loss up to 237 ºC and hence the crystal is thermally stable up to 237 ºC. It is observed that the maximum weight loss is in the temperature range 225 ºC - 380 ºC compared with subsequent stages. A total weight loss of about 75.9 % was observed only at 600 ºC for Ni^{2+} doped ZTS.

It is concluded that the thermal stability of ZTS slightly decreases with the doping of Cd^{2+} and Ni^{2+}. There is no phase transition till the material melts, this increases the temperature range for the use of crystal for NLO application. All the grown crystals, the absence of water in molecular structure was confirmed by the absence of weight loss around 100 ºC. There is no decomposition up to melting point indicating the high thermal stability of material.

4.5 Mechanical studies

Mechanical properties of solids are connected with their structure and other physical and chemical properties and play an important role for practical applications of materials. Among the various experimental tools for the determination of mechanical properties, hardness testing is frequently used to study the mechanical properties of solids. This technique has also become increasingly important for industries involved with micromachines, microelectronics and magnetic recording[12]. The measurements were made at room temperature and loads of different magnitudes such as 25, 50 and 100 g were applied. At a particular load at least five indentations were made. The dimension of different indentations produced on a sample at a given load does not differ from their average value by more than 1 %. To avoid surface effects during microhardness measurements the separation between neighboring indentations was kept more than thrice the diagonal length of indentation impression. The dimensions of both diagonals of an indentation were measured and the average dimension d was calculated from all diagonals made at a particular load P.

Static indentations were made on (100) plane of pure and metal ions doped ZTS crystals using a

Vicker's indenter for various loads. The hardness number of the grown crystals have been calculated using the relation H_v=1.8544 (P/d^2) kg/mm^2 where H_v is the Vicker's hardness number, P is the applied load in kg and d is the average diagonal length of the indented impression in mm. In this study, H_v increases with load up to 50 g and becomes load independent for P=55 g, which can be attributed to the work hardening of the surface. Above 55 g load, significant cracks were observed which may due to the release of internal stresses generated with indentation (Fig. 6). The doping is increasing the strength of the material by showing high resistance to the motion of dislocation compare to pure material. In all the grown crystals, the hardness increases with the increase in applied load (P) and hence it refers to reverse indentation size effect (RISE). The increase of hardness number with load will be useful for nonlinear optical applications.

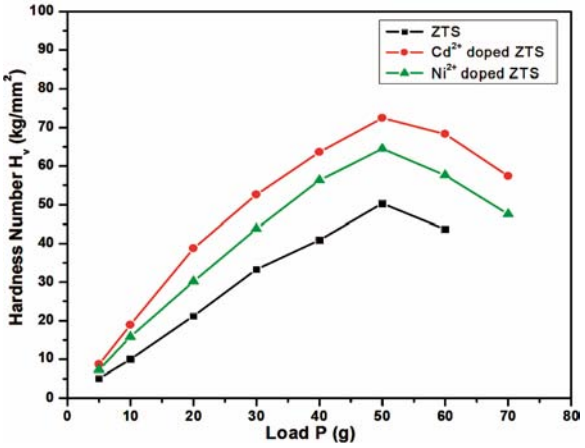

Fig. 6 – Vicker's microhardness of the grown crystals

4.6 Optical studies

Good optical transmittance and lower UV cutoff wavelengths are very important properties for NLO crystals[13]. Optical transmittance spectral analysis of the grown crystal was carried out between 200 and 900 nm is shown in the Fig. 7. It is clear from the spectra that the percentage of optical transmission for pure ZTS crystal is 73% at 800 nm and it increases for Ni (82%) doped ZTS crystals. But the percentage of optical transmission decreases with Cd doping (70%). All of them have sufficient transmission in the entire visible region. Absorption in the near ultraviolet region arises from electronic transitions associated within the sample. This is one of the most desirable properties of the grown crystals for the device fabrication. From the *UV-Vis* spectrum of ZTS, it is noted that there is a maximum transmittance in the entire visible region, which enables it to be a potential candidate for optoelectronic applications.

The band gap energy (E_g) can be calculated directly from the UV cut-off wavelength by using the relation $E_g = hc/\lambda_{(cut)}$ eV where E_g is band gap energy, $h = 6.626\times10^{-34}$ J/s, $c = 3\times10^8$ m/s , $\lambda_{(cut)}$ is the UV cut-off wavelength. The band gap energies were found to be from 4.613 eV to 4.647 eV. The pure and doped ZTS crystals were identified to be wide band gap material.

4.7 Second harmonic generation efficiency (SHG) studies

The second harmonic generation (SHG) efficiency was determined using powder technique developed by Kurtz and Perry[14]. For the SHG efficiency

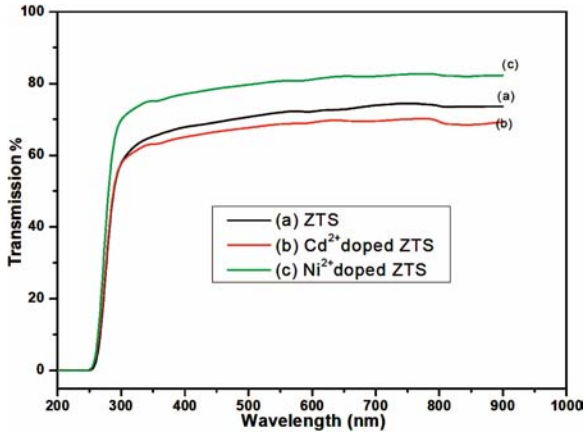

Fig. 7 – UV-Visible transmission spectra of (a) ZTS, (b) Cd^{2+} doped ZTS and (c) Ni^{2+} doped ZTS crystals

measurements, the output of a Q-switched, mode-locked Nd:YAG laser was used to generate about 2.8 mJ/pulse at 1064 nm fundamental radiation. A single shot mode of 8 ns laser pulse at a repetition rate of 10 Hz with a spot radius of 1 mm was used. This experimental set up used a mirror and 50/50 beam splitter to generate a beam with pulse energies of about 2.8 mJ. The input laser beam was allowed to pass through an IR reflector and then directed on the micro-crystalline powdered sample packed in a capillary tube of diameter 0.154 mm. The photodiode detector and oscilloscope arrangement measured the light emitted by the sample. For the Nd:YAG laser, the fundamental beam of 1064 nm generates second harmonic signal of 532 nm (green light). The output pulses measured for ZTS and metal ions doped ZTS are given in Table 2.

The enhancement of SHG efficiency for the doped ZTS crystals are due to the presence of metal ions

Table 2 – SHG output signal voltages of pure and metal ions doped ZTS crystals

Samples	$I_{2\omega}$ (mV)	SHG efficiency
ZTS crystal	18	1.00
Cd^{2+} doped ZTS	20	1.11
Ni^{2+} doped ZTS	21	1.17

which may get added into the structure and increases its non-centrosymmetry and hence increasing its SHG efficiency of ZTS crystal.

5 Conclusions

Optical quality single crystals of pure zinc tris-thiourea sulphate and divalent metal ions doped ZTS were grown from aqueous solution by slow evaporation technique. Single crystal X-ray diffraction confirms that there is no change in basic structure of ZTS while doping. It is confirmed that the grown crystals belong to orthorhombic structure. The prominent well-resolved peak at specific 2θ diffraction angle reveals the high crystalline perfection. FTIR spectral studies confirm the presence of all functional groups of pure and doped ZTS crystals. SEM-EDX analysis confirms the presence of metal ions ($Cd^{2+}$and Ni^{2+}) in the doped ZTS crystals. TGA/DTA analysis shows that the grown crystals have very good thermal stability. Vicker's Microhardness studies showed that hardness number (H_v) increases with the increase of load. Vickers hardness studies reveal that the grown crystals show reverse indentation size effect. UV-Visible study shows that grown crystals have wide range of transparency in the UV and entire visible region and cut-off wave lengths were measured. The SHG efficiency increases to 1.11 times for Cd^{2+} doped ZTS crystal and 1.17 times for Ni^{2+} doped ZTS crystal as compared with pure ZTS crystal. Thus, it is concluded that 1 mol% divalent metal ions doped ZTS crystal will be suitable for optoelectronics applications.

Acknowledgements

The authors acknowledge SAIF, IIT Madras for XRD analysis, Prof. P K Das, Department of Inorganic and Physical Chemistry, IIS, Bangalore, India, for SHG/NLO efficiency measurements, Department of Chemistry, Annamalai University for UV visible spectral studies, Centre for Nano Science and Technology, Anna University, Chennai for TGA/DTA studies. The authors acknowledge VIT University for powder XRD studies.

References

1 Venkatramanan V, Dhanaraj G, Wadhawan V K, Sherwood J N & Bhat H L, *J Cryst Growth*, 154 (1995) 92.
2 Dhumane N R , Hussaini S S, Nawarkhele V V & Shirsat M D, *Cryst Res Technol,* 41 (2006) 897.
3 Long X, Wang G & Han T P J, *J Cryst Growth,* 249 (2003) 191.
4 Ramajothi J & Dhanuskodi S, *Cryst Res Technol,* 38 (2003) 986.
5 Muthu K, Chandrasekaran C, Parthiban S, Meenakshisundaram S P, Bhagavannarayana G & Mojumdar S C, *J Therm Anal Calorim*, 100 (2010) 793.
6 Bhagavannarayana G, Kushwaha S K, Meenakshisundaram S P & Parthiban S, *J Cryst Growth*, 311 (2009) 960.
7 Parthiban S, Murali S, Madhurambal G, Meenakshisundaram S P & Mojumdar S C, *J Therm Anal Calorim,* 100 (2010) 751.
8 Bhagavannarayana G, Chandrasekaran C, Meenakshisundaram S P & Parthiban S, *Cryst Eng Commun,* 11 (2009) 1635.
9 Andreetti G D, Cavalca L & Musatti A, *Acta Crystallogr Sec B*, 24 (1968) 683.
10 Ushasree P M, Jayavel R, Subramanian C & Ramasamy P, *J Cryst Growth,* 197 (1999) 216.
11 Kanagasabapathy K & Rajasekaran R, *Optik,* 124 (2013) 4240.
12 Sangwal K, Surowska B & Blaziak P, *Mater Chem Phys,* 77 (2002) 511.
13 Balakrishnan T & Ramamurthy K, *Spectrochim Acta A*, 72 (2009) 269.
14 Kurtz S K & Perry T T, *J Appl Phys,* 39 (1968) 3798.